

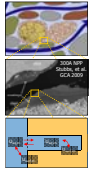
Understanding Grain-Scale Diffusion Processes and Quantifying Mass Transfer Parameters in Hanford 300A Sediments

Michael B. Hay¹, Deborah L. Stoliker¹, James A. Davis¹, and John M. Zachara^{2*}

¹U.S. Geological Survey, Menlo Park, CA 94025; ²Pacific Northwest National Laboratory, Richland, WA 99354

Introduction and Objective

- U(VI) mobility in contaminated aquifers is often controlled by adsorption to mineral surfaces. While the chemical sorption step is rapid (reaching equilibrium within hours), sediments from the Hanford 300A area exhibit slow U(VI) desorption with 100-1000 hours required for equilibrium in batch experiments.
- This kinetic limitation is believed to be the result of a sub-grain scale diffusion process – diffusion of U(VI) into grain fractures, clay aggregates, and clay coatings, where it can adsorb to interior surfaces.
- Predicting migration of the 300A contaminant plume will require an accurate description of grain-scale diffusion, as well as chemical adsorption. But complete understanding of intragrain diffusion is complicated by multiple factors: pore-network heterogeneity, aqueous and surface-phase U(VI) speciation, and the nature of the diffusion process (aqueous-phase vs. diffusion along surfaces).
- Our goal is to study these confounding elements individually in order to gain a better understanding of the whole system.



Objectives

- 1) Characterize the grain-scale physical diffusion regime in 300A sediments.
 - High resolution non-reactive tracer experiments to study diffusion in the absence of complicating chemical factors. Batch- and column-scale experiments using tritiated water (³H₂O) and bromide (Br⁻) as tracers.
 - Multi-rate mass transfer models applied to extract diffusion parameters (diffusion rates and pore volumes).
- 2) Systematically study the effects of aqueous chemistry and surface charge on U(VI) diffusion/desorption.
 - U(VI) adsorption/desorption experiments using ideal porous sorbents exhibiting simple, uniform intragrain pore structures.
 - Diffusion modeling based on actual physical characteristics of the model sorbents to resolve effects of chemical speciation and anion exclusion, and the type of diffusion mechanism (aqueous vs. surface-phase).

Approach

Sediment Experiments

Batch and column experiments were performed with Hanford vadose zone sediments collected from underneath former process ponds in the 300A Area.

Batch:

- ~2mm sediment contacted with tracer spiked artificial groundwater (AGW = ³H or Br⁻) for 2 days to 9 months.
- Tracer-AGW was removed by repeated centrifuging, decanting, and backfilling with AGW ("washing stage").
- Backfill solution was sampled over time as tracer diffused out of intragrain space ("release stage").

Columns:

- 300A <2mm sediment packed in columns. Tracer-AGW pumped in while sampling effluent. Flow periodically stopped for hours to weeks; concentrations rebounded as tracer diffused from intragrain space.

Modeling

Mass balance ($\partial N = 0$ in both models):

$$\frac{\partial}{\partial t} \left(\rho_s \frac{\partial C_s}{\partial x} + \rho_s \frac{\partial C_{s,i}}{\partial x} \right) + \frac{\partial}{\partial x} \left(\rho_s \frac{\partial C_s}{\partial t} + \rho_s \frac{\partial C_{s,i}}{\partial t} \right) = \rho_s \frac{\partial C_s}{\partial x} + \rho_s \frac{\partial C_{s,i}}{\partial x}$$

First-order, multi-rate mass transfer:

$$\frac{\partial C_s}{\partial t} = \sum_{i=1}^n k_i (C_{s,i} - C_s) \quad R = 1 - (1 - \frac{k_i}{k_{i+1}})^{k_{i+1}}$$

Bromide, tritium (no proton exchange): $K_D = 0$
 Including ³H-³H surface exchange: $K_D \neq 0$
 → Calculated based on exchangeable H⁺ concentration

Solved numerically using implicit finite difference. Forward model was iteratively run using UCODE to fit data and obtain mass transfer parameters.

Two mass transfer schemes used to fit tracer curves:

Two-rate model
 Four parameters: $\rho_s, \rho_b, \theta, \theta_{int}, \theta_{ext}$

Lognormal distribution model
 Three parameters: $\theta_{int}, \theta_{ext}, \sigma$

Cumulative lognormal distribution function was discretized to obtain mass transfer coefficients:

$$c_b(t) = \frac{1}{\sigma \sqrt{2\pi}} \int_0^t \frac{1}{\rho_s} \left[\frac{\rho_b}{\rho_s} \frac{1}{\sqrt{2\pi}} \exp\left(-\frac{1}{2} \left(\frac{t-t'}{\tau}\right)^2\right) dt' \right]$$

Diffusion from a sphere modeled using the multi-rate mass transfer coefficients, k_i and θ_{int} calculated from*

$$k_i = \frac{D_i}{r^2} \left(\frac{\theta_{int}}{\theta_{ext}} \right)^2$$

(*Haggerty and Gorelick, WRR 1995)

Proton Exchange

To subtract out the effect of tritium exchange on surface hydroxyls, the exchangeable proton concentration was measured in separate batch experiments.

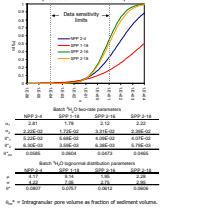
A similar batch procedure was used, with the washing stage replaced by freeze-drying for 1 week at <1 mTorr pressure.

Tracer Diffusion in Batch

Tritium Results

- Data fits were obtained using a multi-rate model with two rates and a lognormal distributed-rate model.
- The majority of the tracer diffusion was fast, with most of the mass released during the washing stage.
- Optimizations of the LND model resulted in wide distributions, with tails falling outside data sensitivity limits (rates too fast or too slow to contribute to observed data).

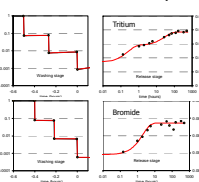
Lognormal cumulative distribution functions



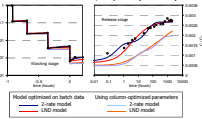
Including Proton Exchange

Model	θ_{int}	θ_{ext}	σ
NPP 2-4, Two-rate	0.000	0.000	0.000
NPP 2-4, LND	0.000	0.000	0.000
SPP 1-18, Two-rate	0.000	0.000	0.000
SPP 1-18, LND	0.000	0.000	0.000

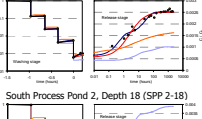
Tritium vs. Bromide Comparison



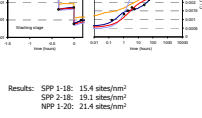
North Process Pond 2, Depth 4 (NPP 2-4)



South Process Pond 2, depth 16 (SPP 2-16)



South Process Pond 2, Depth 18 (SPP 2-18)



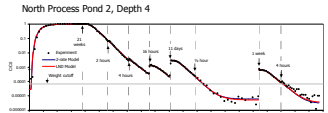
Results: SPP 1-18: 15.4 sites/cm²
 SPP 2-18: 19.1 sites/cm²
 NPP 1-20: 21.4 sites/cm²

Model reoptimization for all sediments is underway. An example of the exchange effect is shown for NPP 2-4 using a value of 18 sites/cm².

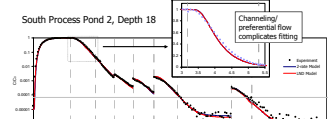
Proton exchange can account for 20-40% of the observed tritium release; results dependent on whether sites are placed in mobile or immobile zone.

Tracer Diffusion in Columns

Tritium Results



South Process Pond 2, Depth 18



Batch vs. Column Comparison

- Two-rate and lognormal distribution models were fit to the column data using a 1/ t^2 weighting scheme. Both models provide good fits to stepoffs.
- Channelling was observed in some columns (SPP 2-16, SPP 2-18), limiting model convergence.
- The optimized lognormal distributions describing mass transfer are wide, with tails falling outside the limits of data sensitivity.

Lognormal cumulative distribution functions (Note the WIDE distributions)

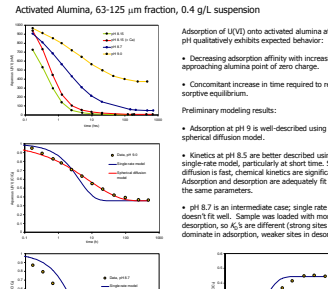
Model	θ_{int}	θ_{ext}	σ
NPP 2-4, Two-rate	0.000	0.000	0.000
NPP 2-4, LND	0.000	0.000	0.000
SPP 1-18, Two-rate	0.000	0.000	0.000
SPP 1-18, LND	0.000	0.000	0.000
SPP 2-16, Two-rate	0.000	0.000	0.000
SPP 2-16, LND	0.000	0.000	0.000
SPP 2-18, Two-rate	0.000	0.000	0.000
SPP 2-18, LND	0.000	0.000	0.000

U(VI) on Model Phases

Model Porous Phases

- Desired characteristics:
- Large grain size to maximize diffusion path length
 - Narrow pore/pore throat diameter
 - Narrow distribution of pore sizes
 - Surface chemistries analogous to mineral phases in Hanford sediments
- Currently using off-the-shelf chromatography substrates:
- 1) Davil® Silica Gel, 0.25-0.5 mm
 - 2) Activated Alumina, 0.1 mm grain size
- N₂ gas adsorption characteristics:
- | Surface area: | 400 cm ² /g |
|---------------------|-------------------------|
| Pore volume: | 0.90 cm ³ /g |
| Avg. pore diameter: | 70.3 Å |
- N₂ gas adsorption of wet-sieved fractions:
- | fraction | surf area | pore vol | pore size |
|-----------|-----------|-----------------------|--------------------------------|
| <63 µm | 19% | 158 m ³ /g | 0.21 cm ³ /g 42.6 Å |
| 63-125 µm | 19% | 153 m ³ /g | 0.21 cm ³ /g 50.1 Å |
| >125 µm | 22% | 150 m ³ /g | 0.27 cm ³ /g 56.1 Å |
- Disolution/precipitation a problem in preliminary experiments. Current experiments are being performed in a lower pH regime.
- Stock material has broad size distribution, but wet-sieved fractions have similar physical characteristics.

Preliminary Results



Batch vs. Column Comparison

Adsorption of U(VI) onto activated alumina at varying pH qualitatively exhibits expected behavior:

- Decreasing adsorption affinity with increasing pH approaching alumina point of zero charge.
- Concomitant increase in time required to reach sorptive equilibrium.

Preliminary modeling results:

- Adsorption at pH 9 is well-described using a spherical diffusion model.
- Kinetics at pH 8.5 are better described using a single-rate model, particularly at short time. Since diffusion is fast, chemical kinetics are significant. Adsorption and desorption are adequately fit using the same parameters.
- pH 8.7 is an intermediate case; single rate model doesn't fit well. Sample was loaded with more U for desorption, so K_D is different (strong sites dominate in adsorption, weaker sites in desorption).

Summary and Conclusions

- High-resolution, batch and column non-reactive tracer experiments were performed on sediments from the Hanford 300A Area to characterize grain-scale diffusion properties. Release curves were described using a multi-rate first order mass transfer model.
- Both batch and column experiments were adequately modeled using either a "two-rate" or a lognormal distributed rate model.
- The two-rate model predicted an intragrain porosity (θ_{int}) of ~3% of the sediment volume in batch. Lognormal distribution estimates were larger due to uncertainty in the washing stage and tail-effects of overly wide lognormal distributions.
- However, θ_{int} decreased with inclusion of proton exchange by 20-40%, indicating the importance of this process. Kinetic experiments are underway to estimate the release rate of the exchangeable protons.
- Fitted rates were slower and θ_{int} values were smaller for the column data relative to batch. Fast kinetics in batch contribute to dispersion in columns, not slow rebounds. Column experiments are less sensitive to the fast kinetics.
- Channelling was significant in some columns, complicating diffusion modeling.
- Much smaller intragrain pore volume is predicted with Br⁻. This discrepancy highlights the importance of anion exclusion effects.

Experiments are in progress using synthetic porous phases as an idealized analogue to the more complex natural sediments. These synthetic phases have a more narrow intragrain pore size distribution, allowing for more controlled study of chemical effects on diffusion.

- Preliminary results with U(VI) on activated alumina exhibit expected behavior: With increasing pH approaching the point of zero charge, adsorption affinity (K_D) decreases and time to reach equilibrium increases.
- The slow-kinetic system (pH 9.0) can be modeled using a spherical diffusion scheme, but the fast-kinetic system (pH 8.5) is nearly first-order. Chemical adsorption kinetics may be playing a stronger role in the latter.

Future Research

- Future work will focus on additional experiments and modeling using ideal synthetic porous phases. The ultimate goal is to be able to use these results to validate conceptual models applied to more complex natural sediments.
- Specific tasks:
- Additional experiments with activated alumina, including experiments with different size fractions and desorption under time-varying chemical conditions.
 - Control experiments with non-porous phases to isolate chemical-kinetic factors.
 - Continue similar experiments with silica gel, addressing complications due to dissolution (near pH 9, appropriate background dissolved silica level).
 - Identify additional porous materials (some might require lab synthesis).
 - Develop surface complexation models for porous materials, to be used in experiments with more complex, time-varying aqueous chemistry.
 - Begin developing more mechanistic diffusion models, incorporating pore geometries and surface-charge effects. Use to test mass transfer model applicability and to probe aqueous-phase vs. surface-phase diffusion mechanisms.